Published in "SEPM Special Publication No. 81: 135–151, 2004" which should be cited to reference this work.

CYCLOSTRATIGRAPHIC TIMING OF SEDIMENTARY PROCESSES: AN EXAMPLE FROM THE BERRIASIAN OF THE SWISS AND FRENCH JURA MOUNTAINS

ANDRÉ STRASSER
Department of Geosciences, University of Fribourg, Pérolles, CH-1700 Fribourg, Switzerland
e-mail: andreas.strasser@unifr.ch
HEIKO HILLGÄRTNER
Shell International Exploration and Production BV, Volmerlaan 8, NL-2280 AB Rijswijk, The Netherlands
e-mail: heiko.hillgartner@shell.com
AND
JEAN-BRUNO PASQUIER
GéoVal Ingénieurs-Géologues SA, Rue de la Majorie 8, CH-1950 Sion, Switzerland
e-mail: jbpasquier@bluewin.ch

Abstract: The Berriasian Pierre-Châtel Formation in the Swiss and French Jura Mountains is dominated by shallow-marine carbonates that overlie lacustrine and marginal-marine sediments with a major transgressive surface. Detailed facies analysis of five sections allows the definition of elementary and small-scale depositional sequences, which commonly exhibit deepening–shallowing trends. Benthic foraminifera and rare ammonites on the platform, as well as a sequence-stratigraphic correlation with a well-dated deeper-water section, furnish the biostratigraphic framework. Thus, the large-scale sequence boundaries below and at the top of the Pierre-Châtel Formation can be correlated with dated boundaries in other European basins. This time constraint and the hierarchical stacking pattern on the platform as well as in the basin suggest that the sea-level fluctuations influencing the formation of the depositional sequences were controlled, at least partly, by Milankovitch cycles. The elementary sequences correspond to the 20 ky precession cycle, and the small-scale sequences to the 100 ky eccentricity cycle.

Uncertainties in the definition of sequences exist if facies contrasts are too low to develop clearly marked sequence boundaries or maximum-flooding intervals. Nevertheless, a best-fit solution for the correlation of the small-scale sequences between the studied sections can be proposed. The lowermost three small-scale sequences of the Pierre-Châtel Formation are analyzed in detail. They are decompacted and correlated on the level of the elementary sequences. Within this relatively precise time frame, the flooding of the Jura platform (following the early Berriasian sea-level lowstand) can be monitored. It is seen that the transgression occurred stepwise: every 20 ky, a transgressive pulse established marine facies farther towards the platform interior.

This study demonstrates that the cyclostratigraphical approach makes it possible to construct a narrow time frame, within which the rates of sedimentary, ecological, and diagenetic processes can be evaluated, phases of differential subsidence identified, and the durations of stratigraphic gaps estimated. The complex and dynamic evolution of an ancient carbonate platform can thus be studied with a time resolution of 20 to 100 ky.

INTRODUCTION

The correct evaluation of time is an everlasting quest in the geological sciences. In the Holocene, several dating methods (e.g., ^{14}C, dendrochronology) are available that allow reaching time resolutions of a few tens of years to a single year. Further back in the geologic past, the error margins of radiometric dating increase and reach values on the million-year scale (Berggren et al., 1995). In order to estimate the rates of sedimentological processes in the past (such as sediment production and accumulation, diagenesis, ecological changes), a much higher precision is needed. It is useless to just divide the thickness of the stratigraphic column by the corresponding time interval when calculating sedimentation rates: these rates are facies dependent, time may be condensed in hiatuses, sediment production rates may have been much higher than the final accumulation, and differential compaction may have distorted the sedimentary record.

Cyclostratigraphy allows constructing a relatively precise time scale in the geologic past even though radiometric dating gives large error margins (e.g., Schwarzacher, 1993; Lourens et al., 1996). If detailed analysis of the sedimentary record demonstrates that the formation of depositional sequences ("sedimentary cycles") is related to the quasi-periodic perturbations of the Earth's orbit (Milankovitch cycles), then a time resolution of 20–100 ky can potentially be reached. This time frame is comparable to that of the Pleistocene and Holocene, where the parameters controlling sedimentary processes are better known.

Detailed analyses of facies and stacking pattern in Berriasian (lowermost Cretaceous) shallow-water, carbonate-dominated sequences in Switzerland and France have shown that sedimentation was controlled at least partly by Milankovitch cycles (Pasquier, 1995; Pasquier and Strasser, 1997; Strasser and Hillgärtner, 1998; Hillgärtner, 1999). It appears that sea-level fluctuations were the most dominant parameter but that climatic changes controlling nutrient and siliciclastic fluxes, and synsedimentary tectonics shaping the substrate, also were important in determining facies distribution. Elementary sequences (the smallest units where facies evolution indicates an environmental cycle) formed in tune with the 20 ky precession cycle. Elementary sequences stack into small-scale and medium-scale sequences, representing the 100 ky and 400 ky eccentricity cycles, respectively. Sequences corresponding to the obliquity cycle of 40 ky could not be identified. Large-scale sequences are composed of several medium-scale sequences and mostly reflect tectono-eustatic changes.

Cyclostratigraphy: Approaches and Case Histories
SEPM Special Publication No. 81, Copyright © 2004
SEPM (Society for Sedimentary Geology), ISBN 1-56576-108-1, p. 135–151.

In the present paper, the focus is on the detailed analysis of the record of a large-scale transgression, which flooded a shallow platform. Within a biostratigraphic and sequence-stratigraphic framework, cyclostratigraphy is used to monitor this transgression with time steps corresponding to the 20 ky of the orbital precession cycle.

GEOGRAPHIC AND PALEOGEOGRAPHIC SETTING

Five shallow-water sections are situated in the Swiss and French Jura Mountains, and a deeper-water section used for biostratigraphic and cyclostratigraphic calibration is located in the Vocontian Basin in France (Fig. 1). In the Early Cretaceous, the Jura platform was part of the complexly structured northwestern margin of the Ligurian Tethys, and the Vocontian Basin represented a dead-end branch of this ocean (Fig. 2). The study area in the Jura was situated at a latitude of about 32 to 33° N (Dercourt et al., 2000). Paleoenvironmental conditions were subtropical and ideal for extensive carbonate production on the shallow platform. In the Vocontian Basin, hemipelagic and pelagic carbonate sedimentation was active but carbonate mud was also shed from the adjacent platforms (Hillgärtner, 1999).

During the latest Jurassic and earliest Cretaceous, a slowdown of sea-floor spreading in the western Tethys and accelerated rifting in the North Atlantic (Late Cimmerian phase; Sinclair et al., 1994) led to thermal doming and a long-term tectonoeustatic sea-level fall, which caused widespread emergence of the Armorican, Central, and Rhenish–Bohemian massifs (Fig. 2; Ziegler, 1988). This, together with episodically increased rainfall, furnished siliciclastics to platform and basin. Block faulting and differential subsidence affected the Jura platform and the Vocontian domain (Wildi et al., 1989; de Graciansky and Lemoine, 1988) and caused a very heterogeneous facies distribution, especially on the shallow platform.

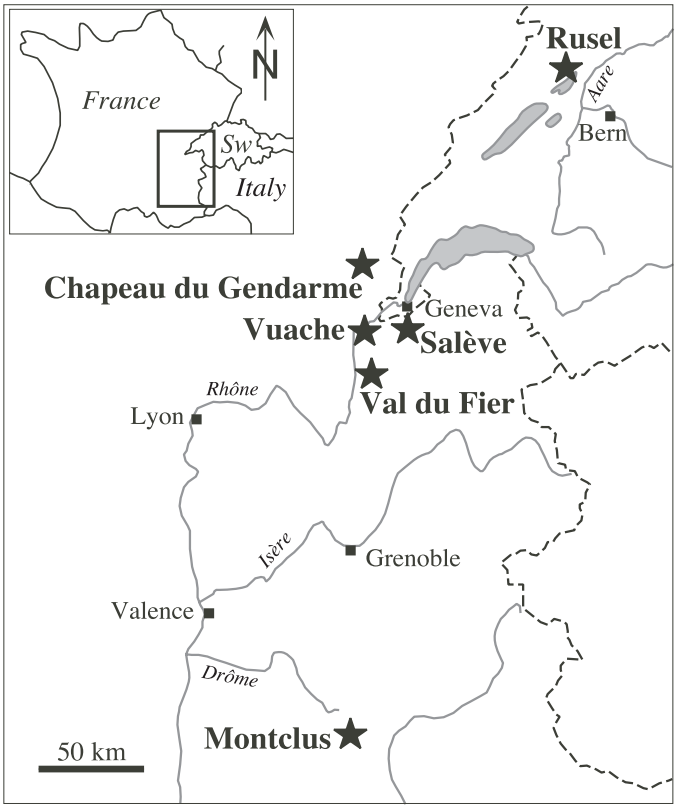

FIG. 1.—Location of the studied sections in Switzerland (Sw) and France.

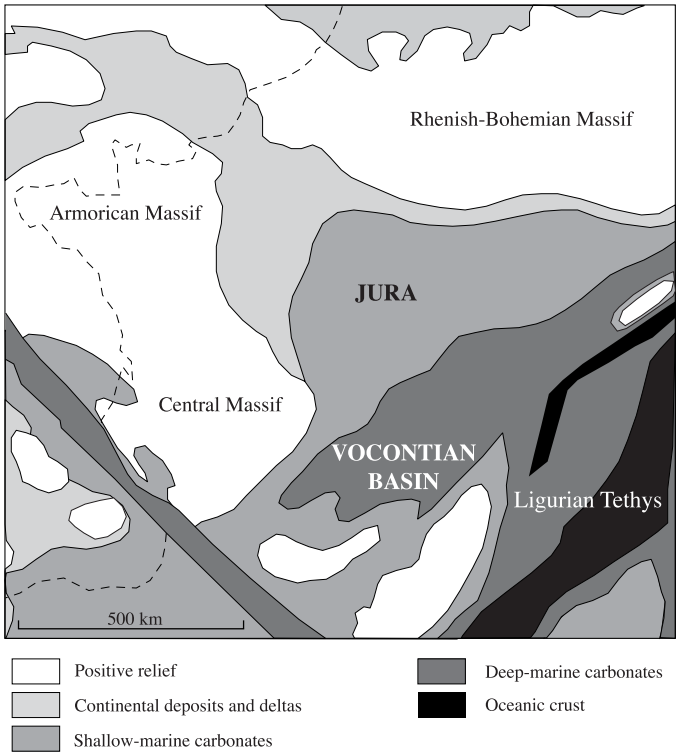

FIG. 2.—Paleogeography in the Early Cretaceous, including the shallow Jura platform and the Vocontian Basin (based on Ziegler, 1988).

Following the Alpine orogeny, the Jura Mountains were faulted and folded, the main tectonic activity going on during the late Miocene–early Pliocene. Overburden was a few hundred meters in the north and about 2000 m in the southern French Jura (Trümpy, 1980). For the present study, no palinspastic reconstructions were undertaken. The distances between the studied sections would have to be stretched by a few kilometers in a north–south direction, and some sections would be offset by a few kilometers by north–south-trending faults (Meyer, 2000). However, the general order on the transect from inner platform in the north (Rusel section; Fig. 1), central and outer platform (Chapeau-du-Gendarme, Vuache, Val-du-Fier, and Salève sections), and basin (Montclus section) in the south has not changed. The Salève section contains massive ooid grainstones that represent high-energy shoals typical of platform margins. On the transect, this section is therefore placed in the corresponding position, and the Val-du-Fier section in a more protected location. It is assumed that the platform margin was not a straight line but displayed promontories and bays.

LITHOSTRATIGRAPHIC AND BIOSTRATIGRAPHIC FRAMEWORK

In the platform sections, the studied interval comprises the top of the Goldberg Formation, the Pierre-Châtel Formation, and the base of the Vions Formation (Fig. 3). The Goldberg Formation (defined by Häfeli, 1966) displays to a large part the "Purbeckian"

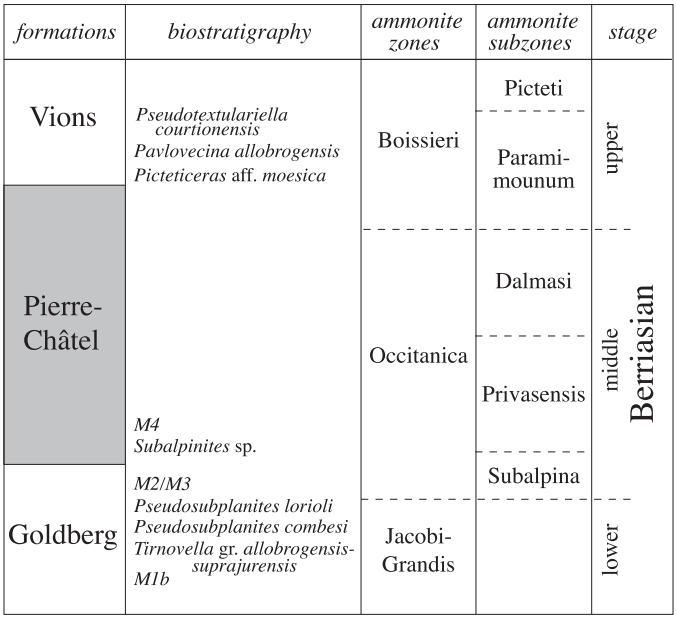

FIG. 3.—Lithostratigraphy, biostratigraphy, and chronostratigraphy of the studied interval (biostratigraphy of ammonites and benthic foraminifera according to Clavel et al., 1986; charophyte–ostracod assemblages M1b, M2, M3, and M4 according to Détraz and Mojon, 1989).

facies: peritidal carbonates with charophytes, black pebbles, and, locally, evaporite pseudomorphs (Strasser, 1988). The top of this formation is locally eroded and condensed, which can be explained by differential subsidence and uplift due to enhanced tectonic activity during the Early Cretaceous (De Graciansky and Lemoine, 1988). The Pierre-Châtel Formation was defined by Steinhauser and Lombard (1969). Its base represents a rapid flooding of the partly emergent Purbeckian platform, and its bulk is made up of shallow but normal-marine carbonates (Pasquier, 1995). The overlying Vions Formation (Steinhauser and Lombard, 1969) displays mainly shallow-marine facies but also contains lacustrine and palustrine levels. Furthermore, it is characterized by abundant detrital quartz and clays (Hillgärtner, 1999).

Dating of these formations is difficult because biostratigraphically relevant fossils are rare. Clavel et al. (1986) described ammonites at the top of the Goldberg Formation, at the base of the Pierre-Châtel Formation, and at the base of the Vions Formation. The base of the Pierre-Châtel Formation can thus be attributed to the Subalpina Subzone and its top to the Paramimounum Subzone (Fig. 3). The foraminifer *Pavlovecina allobrogensis* (commonly associated with *Pseudotextulariella courtionensis*) typically appears in the Paramimounum Subzone (Clavel et al., 1986). Charophyte–ostracod assemblages have been defined by Détraz and Mojon (1989) and are calibrated on ammonite zones. Thus, even in the absence of ammonites, these associations allow constraining the studied interval. In the Montclus section of the Vocontian Basin, ammonites and calpionellids are abundant and a good biozonation is available (Le Hegarat, 1971).

MATERIAL AND METHODS

The platform sections were logged and sampled in considerable detail. The Rusel section is based on work by Pasquier (1995), and the Chapeau-du-Gendarme section has been analyzed by Waehry (1989) and Hillgärtner (1999). The Vuache section was first described by Blondel (1984) and was studied again by Hillgärtner (1999). The section of Val du Fier is based on work of Darsac (1983) and Hillgärtner (1999). The Salève outcrop was studied by Waehry (1989), Strasser and Hillgärtner (1998), and Hillgärtner (1999). The depositional environments and their evolution through time have been interpreted from the analysis of microfacies, sedimentary structures, and bedding surfaces. A high-resolution sequence-stratigraphic interpretation is made where facies evolution allows identification of accommodation changes. The sequence-stratigraphic terminology follows Vail et al. (1991).

An example of this approach is given in Figure 4. On the shallow platform, rapid loss of accommodation leading to the development of a sequence boundary is indicated by lacustrine or tidal-flat facies, and by birdseyes. Because of lack of accommodation, lowstand deposits are not developed or only thinly developed, or reworked within early transgressive deposits. The transgressive surface is commonly underlain by reworked material, including black pebbles indicative of subaerial exposure (Strasser and Davaud, 1983). Relatively deepest or most open-marine water is indicated by fauna such as echinoderms or brachiopods. Levels with increased bioturbation suggest a reduced sedimentation rate and, when combined with open-marine fauna, are interpreted as intervals of maximum flooding (maximum-flooding surfaces are not always developed). The marly levels can have different origins: clays may be washed into the system during relative sea-level lowstands and thus emphasize sequence boundaries, they can accumulate during maximum flooding when the seafloor is below wave base, or they can be related to increased rainfall in the hinterland (Strasser and Hillgärtner, 1998). The interpretation of the marls must therefore be based on their faunal and floral content, and on the context within the depositional sequence. Two orders of depositional sequences can be distinguished in the example of Figure 4: elementary sequences, consisting most commonly of one bed, and small-scale sequences, composed of three to five elementary sequences.

The deeper-water Montclus section was sampled in less detail because the facies consist mainly of limestone–marl alternations and are relatively homogeneous. The section presented here and its interpretation is based on work by Pasquier (1995), Pasquier and Strasser (1997), Hillgärtner (1999), and Strasser et al. (2000).

The methodology used for the sequence-stratigraphic and cyclostratigraphic interpretation of the studied interval follows several steps (Strasser et al., 1999):

1. Identification of elementary depositional sequences, i.e., of facies evolution through time corresponding to one cycle of environmental change (mainly a deepening–shallowing trend in the platform sections, and a limestone–marl couplet in the basin);
2. Identification of the stacking pattern of elementary sequences that compose small-scale, medium-scale, and large-scale depositional sequences, which again show characteristic facies evolutions (general deepening–shallowing trends on the platform, and upward thinning or upward thickening of the limestone beds in the basin);
3. Sequence-stratigraphic interpretation of the depositional sequences on all scales, independently for each section;
4. Comparison of this interpretation between the sections, and correlation of the sequence-stratigraphic elements to find a best-fit solution that is also compatible with the biostratigraphic framework;

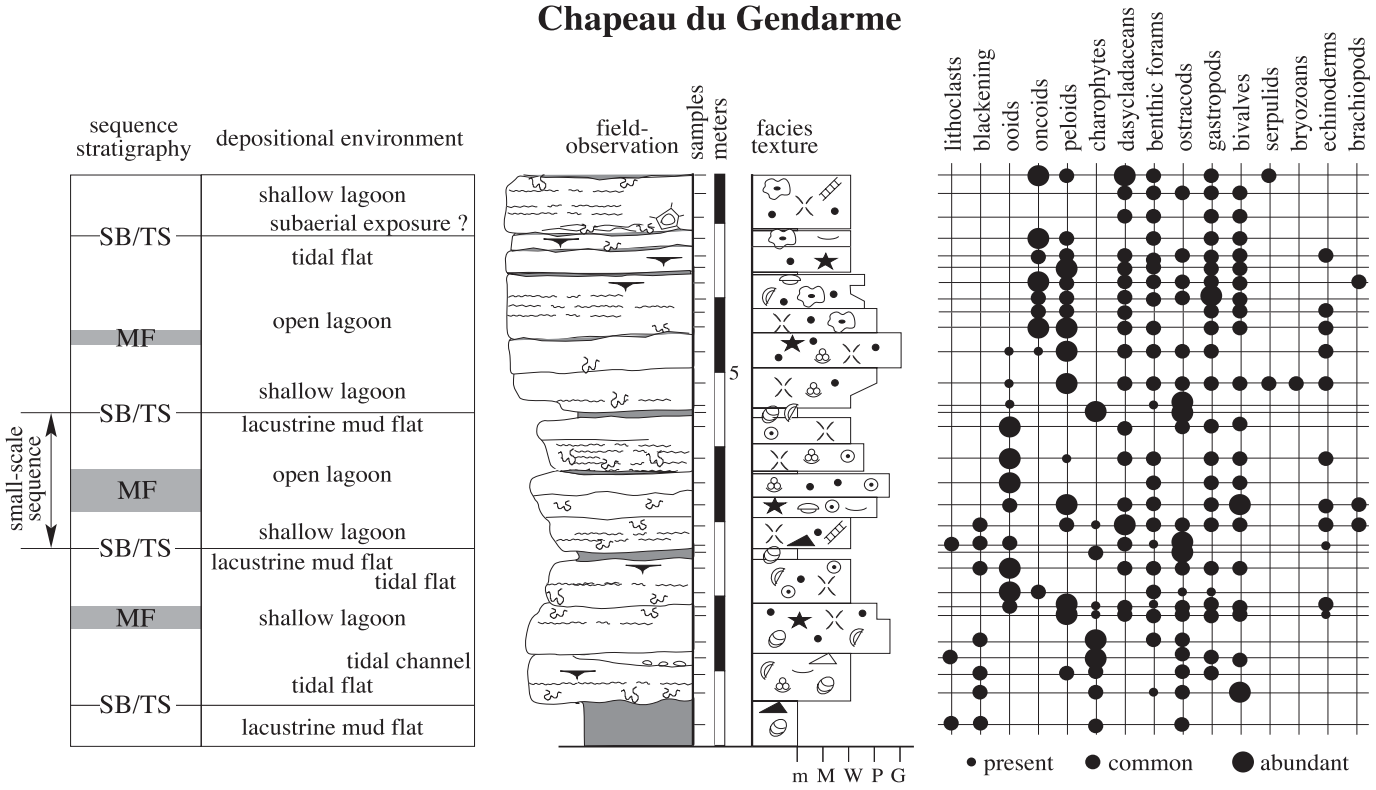

FIG. 4.—Example of detailed facies analysis, and interpretation of depositional environments and easily identifiable sequence-stratigraphic elements (base of Pierre-Châtel Formation, Chapeau-du-Gendarme section; microfacies analysis by Waehry, 1989). Symbols for facies and sedimentary structures as in Figure 5.

5. Comparison of large-scale sequence boundaries with boundaries identified in other sedimentary basins in the same biostratigraphic position;
6. Counting of the elementary and small-scale sequences between dated large-scale sequence boundaries and dated limits of biostratigraphic zones;
7. If the duration of these depositional sequences falls within the Milankovitch frequency band, a cyclostratigraphic time scale can be proposed.

CORRELATION

A best fit-solution of correlation of small-scale sequences between the studied sections is shown in Figure 5. First, the platform sections are discussed, then a correlation with the basinal section of Montclus is attempted.

Platform Sections

The top of the Goldberg Formation exhibits birdseyes, black pebbles, and pedogenetic brecciation (below the transgressive surface at the base of the sections in Fig. 5). The Subalpina Subzone is condensed (Clavel et al., 1986). This indicates prolonged emersion at this level, which is interpreted as a major sequence boundary. According to its biostratigraphic position it can be correlated with sequence boundary Be4 of Hardenbol et al. (1998), which has been recognized also in other European basins.

The base of the Pierre-Châtel Formation is marked by a sharp transgressive surface (TS in Fig. 5). Facies then indicate periodic deepening and shallowing of depositional environments, and/or suggest that conditions changed from restricted marine to open marine and back to restricted. The identification of depositional sequences is relatively easy in the sections representing the platform interior, where facies contrasts are well developed (Rusel, Chapeau du Gendarme; Fig. 5). In the Salève section, however, surfaces within bioclastic and ooid grainstones may well have formed through shoal migration and not through relative sea-level changes. The correlation of several small-scale sequences therefore is uncertain.

In a few cases, it is not clear where the limit of a small-scale sequence should be chosen, because two or more bedding surfaces of elementary sequences show the characteristics of a sequence boundary. This is interpreted to be due to the superposition of high-frequency sea-level fluctuations on a longer-term trend of sea-level evolution (Fig. 6). In this way, not only sequence boundaries but also transgressive and maximum-flooding surfaces may be repeated and define zones that correspond to the time of longer-term sea-level fall, transgression, or maximum flooding, respectively (Montañez and Osleger, 1993). Furthermore, changing amplitudes of the high-frequency fluctuations may attenuate or accentuate such surfaces and zones (Strasser et al., 1999). In Figure 5, sequence-boundary zones of small-scale and large-scale sequences are marked in gray.

In the sections of Rusel, Chapeau du Gendarme, Vuache, and Val du Fier, the small-scale sequences display a general thickening-upward trend. This trend, however, is interrupted by karst surfaces in the first two sections, by vadose cementation and circumgranular cracks indicating pedogenesis at Vuache, and by

several levels of root traces in Val du Fier (sequences 15 to 18, Fig. 5). This apparently rapid loss of accommodation is interpreted as a major sequence boundary. Above, the appearance of the foraminifera *Pavlovecina allobrogensis* and *Pseudotextulariella courtionensis* indicate the Paramimounum Subzone (Fig. 3; Clavel et al., 1986). This major sequence boundary can therefore be correlated with Be5 of Hardenbol et al. (1998). The maximum-flooding interval of the large-scale sequence (defined between Be4 and Be5) is placed where the thickest beds suggest highest accommodation gain and keep-up of the carbonate system (small-scale sequence 16 at Chapeau du Gendarme), or where intense bioturbation points to reduced sedimentation rates because of a low carbonate production in deeper water (middle part of sequence 16 at Salève).

Between the transgressive surface at the base of the Pierre-Châtel Formation and sequence boundary Be5, 6 to 9 small-scale sequences are counted (Fig. 5). However, the correlation across the platform suggests that at Rusel and Chapeau du Gendarme the uppermost sequences are truncated. At Vuache, strong condensation at this level is indicated by the limited extension of *P. allobrogensis* (Hillgärtner, 1999). A fall of eustatic sea level alone cannot explain these features, and faulting of the Jura platform inducing differential subsidence has to be assumed at that time (De Graciansky and Lemoine, 1988; Hillgärtner, 1999).

Basinal Section

In order to better constrain the biostratigraphic guidelines and to better understand the sequential evolution of the platform sections, a correlation with the well-dated Montclus section in the Vocontian Basin was undertaken. There, a major sequence boundary is indicated at the base of an interval containing relatively thick, irregular, and locally channeled limestone beds, which are interpreted as lowstand deposits (Pasquier, 1995; Pasquier and Strasser, 1997). This boundary coincides with the Subalpina–Privasensis Subzone boundary (Le Hegarat, 1971) and can therefore be correlated with Be4 of Hardenbol et al. (1998). The lowstand deposits are overlain by an interval of thinner and more homogeneous limestone–marl alternations, which are thought to represent transgressive deposits. A rapid change to even thinner alternations is interpreted as a second transgressive pulse (TS2, Fig. 5). The marliest part of the section (partly covered in the outcrop) is attributed to a condensed interval (corresponding to the maximum flooding of this large-scale sequence), and the following alternations displaying a thickening-up trend are seen as highstand deposits. A major sequence boundary is placed at the base of the particularly thick limestone bed at meter 22.5, or at the base of a slumped interval (thus defining a sequence-boundary zone). This boundary is situated in the Paramimounum Subzone and corresponds to Be5 of Hardenbol et al. (1998).

The limestone–marl couplets group into bundles of 2 to 6 (Fig. 5). These bundles are interpreted as small-scale sequences, and one couplet as an elementary sequence (Pasquier and Strasser, 1997). The limestone beds are composed to a large part of nannoplankton (Cotillon et al., 1980; Strohmenger and Strasser, 1993). The limits of the small-scale sequences have been chosen at the bases of the thickest limestone beds, because these beds are thought to have formed during lowstand conditions when planktonic productivity was concentrated above the hemipelagic realm while the platform was at least partly exposed. With rising sea level, carbonate productivity was active also on the platform, less nannoplankton was produced in the open ocean, and marly facies formed. However, this oversimplified model was certainly complicated by phases of export of carbonate mud from platform to basin (Schlager et al., 1994; Pittet et al., 2000), by ocean currents, temperature, and nutrients influencing planktonic productivity (Einsele and Ricken, 1991), and by climate- and current-controlled input of clay minerals.

Basin-to-Platform Correlation

Eighteen to 19 small-scale sequences have been identified at Montclus between Be4 and Be5 (Fig. 5). Be4 in the basin correlates well with the top of the Goldberg Formation on the platform, where the Subalpina Subzone is condensed. It is tempting to correlate the transgressive surface TS1 at the top of the lowstand at Montclus with the base of the Pierre-Châtel Formation (TS at Salève; Fig. 5). However, when counting the small-scale sequences downward from Be5, the fit is better if sequence 10 at Montclus is correlated with the first small-scale sequence of the Pierre-Châtel Formation (Fig. 5). This solution implies that the platform already started being flooded while lowstand conditions continued in the basin (Pasquier and Strasser, 1997). In sequence 11, which in the basin is interpreted as following a transgressive pulse, the platform experienced an opening to more marine conditions, which allowed the growth of echinoderms and brachiopods even in the platform interior (Rusel and Chapeau-du-Gendarme sections). Also, it is evident from Figure 5 that nine small-scale sequences constituting the bulk of the lowstand in the basin are missing or strongly condensed on the platform.

It is interesting to note that the large-scale condensed section at Montclus (at the top of small-scale sequence 15) is not isochronous with the maximum flooding defined on the platform within small-scale sequence 16. Apparently, the sedimentary systems in the basin and on the platform reacted differently to the same eustatic sea-level change, or differential tectonic movements caused a shift of the time interval of fastest relative sea-level rise.

In lack of continuous outcrop or seismic profiles that allow tracing of sequences from the platform to the basin, sequence boundaries, transgressive surfaces, and maximum-flooding surfaces have to be identified on the basis of the observations in the individual sections. There, the best-developed surfaces will be chosen, which, however, may be offset by one or two high-frequency sea-level cycles when compared to the theoretical position on the long-term sea-level trend (Strasser et al., 1999). This offset may vary from one section to the other because of differences in basin morphology and/or sediment availability.

CYCLOSTRATIGRAPHY

Building a Time Scale

In the Montclus section, 71 to 104 limestone–marl couplets are counted between Be4 and Be5, depending on considering the thin beds of marly limestone as part of a couplet or as a separate couplet, and on excluding or including small-scale sequence 19 (Fig. 5). According to Hardenbol et al. (1998), Be4 is dated at 141.04 Ma, and Be5 at 139.33 Ma. The high precision of these numbers is of course unrealistic, considering that the Tithonian–Berriasian boundary is dated at 144.2 Ma with an error margin of ± 2.6 Ma (Gradstein et al., 1995). Nevertheless, the time between these two sequence boundaries can be estimated to be in the range of about 1.7 million years.

Assuming that one limestone–marl couplet represents an equal time increment, the duration of one couplet would vary between 24 and 16 ky. The small-scale sequences, on the other hand, would have durations of 90 to 95 ky. These numbers are close to the periodicities of the orbital precession cycle (20 ky in the Early Cretaceous; Berger et al., 1989) and the first eccentricity

FIG. 5.—Best-fit correlation based on the sequence-stratigraphic and cyclostratigraphic interpretation of each section. For discussion refer to text.

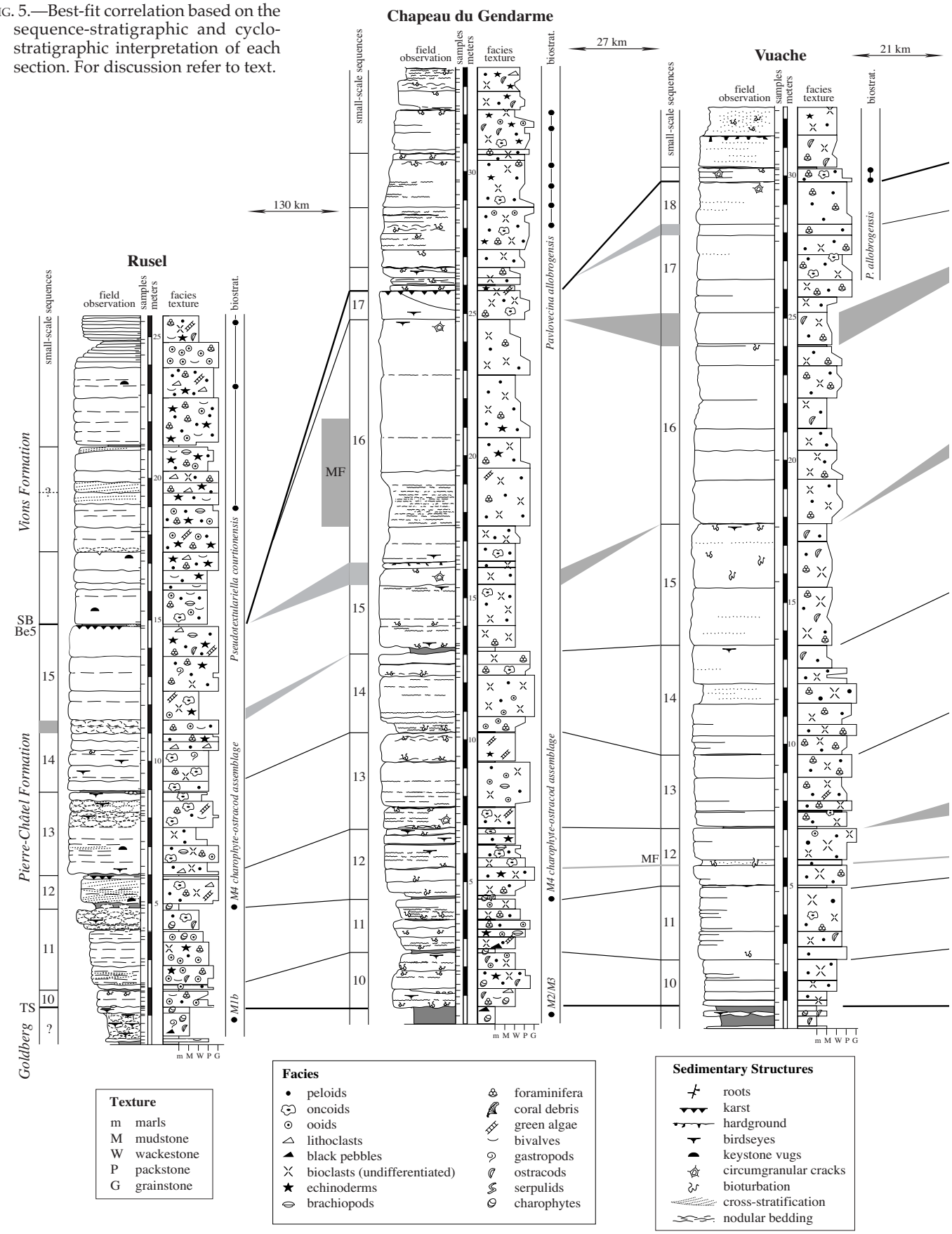

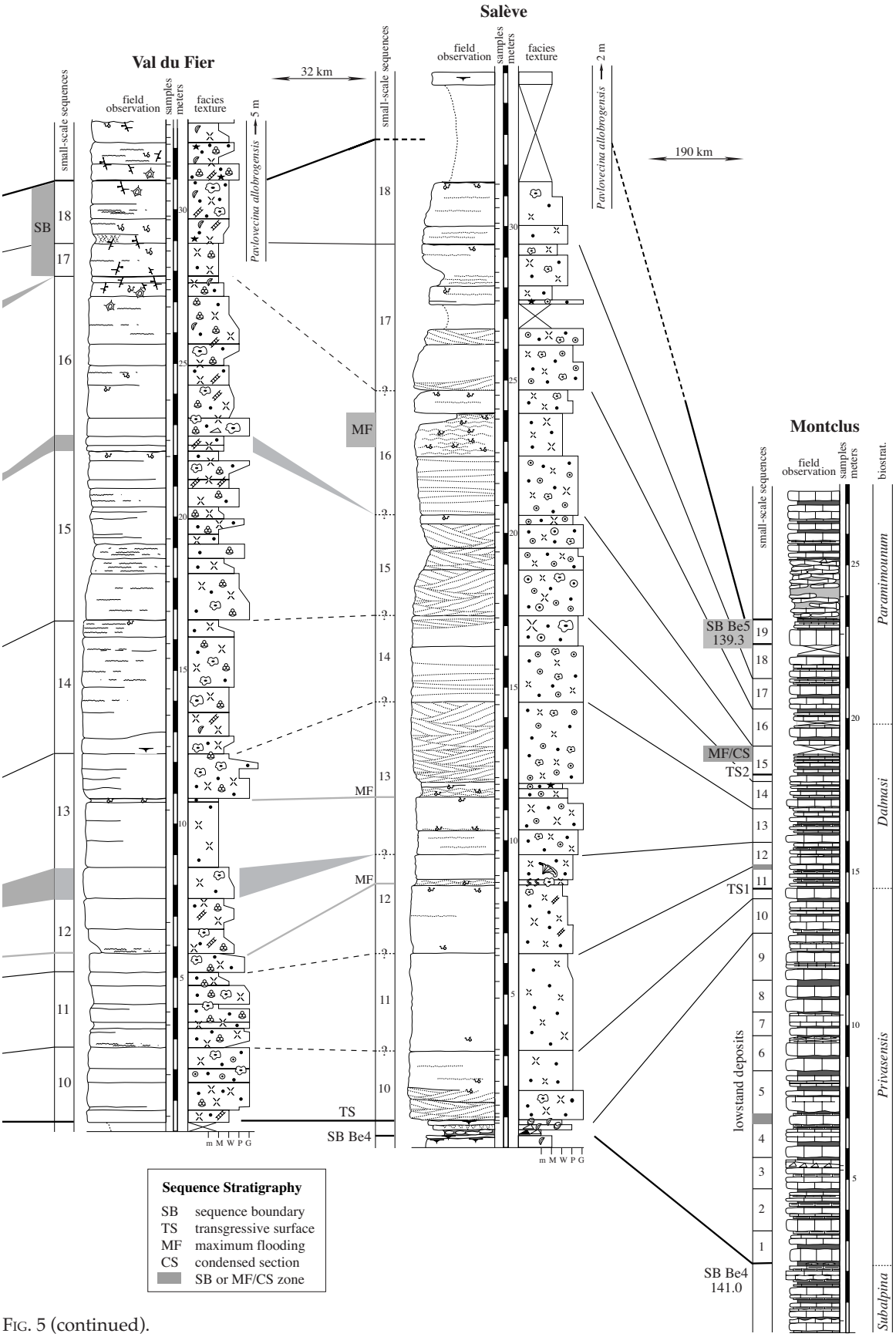

FIG. 5 (continued).

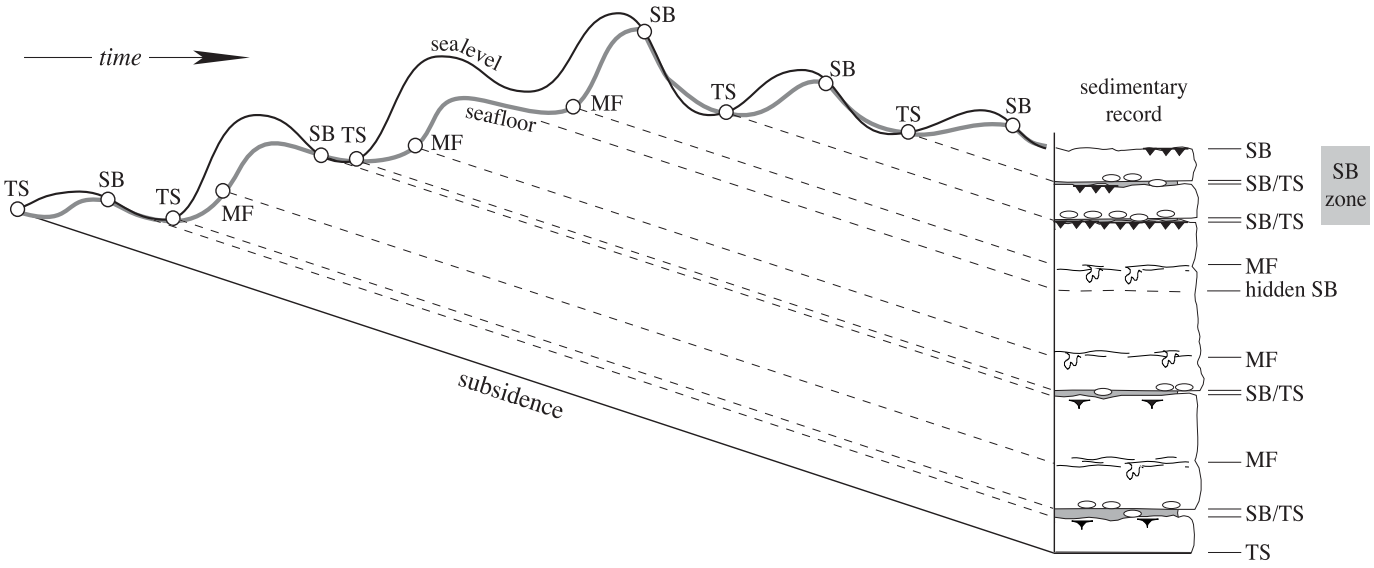

FIG. 6.—Hypothetical depositional sequences formed by high-frequency sea-level fluctuations superimposed on a longer-term rising and falling sea-level trend. Symbols are as in Figure 5. Note that stacked sequence boundaries form a sequence-boundary zone during the falling trend, and that a sequence boundary may not be expressed lithologically on the rising trend ("hidden SB").

cycle (100 ky), respectively. It is therefore implied that the sedimentary record at Montclus formed in tune with environmental changes controlled by insolation changes in the Milankovitch frequency band.

The counting of inferred 20 ky and 100 ky cycles between sequence-stratigraphic surfaces and limits of biozones now allows an improved estimate of time in the sections studied. Figure 7 shows that there are some discrepancies between the interpretation of the Montclus section and the chart published by Hardenbol et al. (1998). At Montclus, the Privasensis Subzone apparently lasted 950 ky, but only 500 ky are given in the chart. The duration of the Dalmasi Subzone, however, is consistent. Hardenbol et al. place the condensed interval of the large-scale sequence (Be4–Be5) at 139.7 Ma in the Paramimounum Subzone, whereas at Montclus it appears in the uppermost Dalmasi Subzone. The duration of the highstand, however, is consistent with 300 to 400 ky. The discrepancies may be due to problems with attributing absolute ages to biozones, and/or by the fact that the best-developed physical expression of a sequence boundary or a maximum-flooding interval does not necessarily occur at the same time in different paleogeographic positions (Jacquin and de Graciansky, 1998).

Hardenbol et al. (1998)					Montclus				platform sections		
stage	*ammonite subzones*	*duration*	*sequence stratigraphy*	*duration*	*ammonite subzones*	*duration*	*sequence stratigraphy*	*duration*	*bio-stratigraphy*	*sequence stratigraphy*	*duration*
Berriasian upper	Parami-mounum		**Be5** 139.33		Parami-mounum		SB		*P. allo-brogensis*	SB	
	140.05		CS 139.7	350 ky				300–400 ky		hiatus	150–250 ky
							CS			MF	
middle	Dalmasi	500 ky		1.35 My	Dalmasi	500 ky		500–600 ky	*M4*		650 ky
	140.55						TS			TS	
	Privasensis	500 ky			Privasensis	950 ky		900–1000 ky		hiatus	
	141.04		**Be4** 141.04				SB				
	Subalpina				Subalpina				*M2/3*	SB	

FIG. 7.—Chronostratigraphy of the studied interval according to Hardenbol et al. (1998), and comparison with the estimation of time based on the cyclostratigraphic analysis of the deeper-water Montclus section and the platform sections. For discussion refer to text.

Timing of the Platform Sections

If the correlation presented in Figure 5 is accepted as a working hypothesis, the small-scale sequences identified in the platform sections would correspond to 100 ky. These sequences are commonly composed of 2 to 6 beds, whereby a bed would correspond to an elementary sequence with a duration of 20 ky. However, in many cases it is difficult to define the limits of the elementary sequences because facies contrasts are too low. Bedding planes can also have formed through autocyclic processes such as shifting mudbanks (Pratt and James, 1986) or through clay input that was not related to sea-level change. In the case of sequence 12 at Rusel, only transgressive shoals are preserved. The karst surface that terminates this small-scale sequence may have formed through a drop of eustatic sea level (Fig. 6) and/or through tectonic uplift in this area.

HISTORY OF A TRANSGRESSION

Decompaction and High-Resolution Correlation

The relatively good time resolution obtained by cyclostratigraphy now permits detailed monitoring of the flooding of the Jura platform. For this purpose, the lowermost three small-scale sequences of the Pierre-Châtel Formation were chosen. The elementary sequences are relatively well defined (at least in the platform-interior sections), and a correlation with a time resolution of 20 ky can thus be proposed. To better understand the sea-level history, however, these sequences first have to be decompacted in order to evaluate the true accommodation changes (Fig. 8).

Mechanical reorganization of grains and dewatering in carbonate mud leads to a porosity loss of 10 to 30% after the first 100 m of burial (Moore, 1989). The experiments of Shinn and Robbin (1983) yielded values of 20 to 70% of volume loss through mostly mechanical and dewatering compaction. These values will be less if carbonate cementation sets in very early (e.g., Halley and Harris, 1979). With deeper burial, chemical compaction becomes important. Burial of over 2 km probably never occurred in the Jura Mountains (Trümpy, 1980) but pressure solution at grain contacts testifies to some dissolution processes in the studied sediments. Goldhammer (1997) proposes a compaction of slightly over 50% for 1 m of carbonate mud buried at 1000 m, and of about 15% for 1 m of carbonate sand at the same burial depth. According to Enos (1991), muddy terrigenous and muddy carbonate sediments do not have significantly different compaction curves. However, pressure solution along clay seams may of course enhance chemical compaction in carbonates (e.g., Bathurst, 1987). On the basis of these published values, the following decompaction factors have been chosen for the present study: 1.2 for grainstones and 2.5 for mudstones. For packstones and wackestones, the intermediate factors 1.5 and 2 are assumed, and for marls the factor 3. These factors are very rough estimates, but the decompacted sections nevertheless give a more realistic impression of the Early Cretaceous sediment accumulations than today's outcrops.

Figure 8 shows the effect of this decompaction and a best-fit solution of correlation on the 20 ky scale for the first three small-scale sequences. In some small-scale sequences, also the maximum-flooding intervals are identified and correlated.

Reconstruction of High-Frequency Eustatic Sea-Level Fluctuations

Reconstruction of the "true" eustatic sea-level changes that controlled sedimentation in the past is of course not possible. An approximation, however, can be proposed if the original sediment thickness, the range of water depth for each facies encountered, and the subsidence rate can be estimated. The first three small-scale sequences of the Chapeau-du-Gendarme section are well suited for such an approximation: they all end with intertidal or lacustrine facies, which sets mean sea level at zero. Maximum flooding of these sequences is indicated by subtidal, normal-marine, bioturbated, and low-energy facies. Water depth there is estimated at a minimum of one meter but could have been considerably more. The elementary sequences are well developed and give the timing of the sea-level fluctuations in 20 ky steps. Farther up in the section, the elementary sequences are less well defined, and intertidal facies are less common. The reconstruction of the sea-level curve therefore becomes very hypothetical (Fig. 9).

It is assumed that the sea-level fluctuations were more or less symmetrical. In the Early Cretaceous, ice in high latitudes and on mountains was probably present but volumes were small (Fairbridge, 1976; Frakes et al., 1992; Eyles, 1993; Price, 1999). Orbitally controlled climatic changes would have resulted in only minor glacio-eustatic sea-level fluctuations. However, insolation changes could also contribute to low-amplitude sea-level fluctuations through thermal expansion and contraction of the uppermost layer of ocean water (Gornitz et al., 1982), thermally induced volume changes in deep-water circulation (Schulz and Schäfer-Neth, 1998), and/or water retention and release in lakes and aquifers (Jacobs and Sahagian, 1993).

In order to accumulate 12 meters of sediment in the 300 ky corresponding to the first three small-scale sequences, accommodation gain must have been 4 m/100 ky on average. For small-scale sequences 13 to 15, 5 m/100 ky is assumed, and sequence 16 required 13 m of accommodation (Fig. 9). Part of the accommodation gain was due to long-term sea-level rise, which led to the general flooding of the Jura platform. However, the thickness variations of the small-scale sequences across the platform (Fig. 5) suggest that differential subsidence significantly influenced accommodation. During the deposition of sequence 16, a rapidly subsiding block was situated at Chapeau du Gendarme, while subsidence was attenuated or even uplift occurred at Rusel. According to Wildi et al. (1989), average subsidence rate on the Jura platform in the Late Jurassic and Early Cretaceous varied between 1 and 7 m/100 ky.

For the first three small-scale sequences of the Pierre-Châtel Formation, the long-term accommodation gain was subtracted from the reconstructed sea-level curve. This results in a high-frequency sea-level signal (Fig. 10). The wavelengths were adjusted slightly to fit the inferred 20 ky cyclicity. The amplitudes are minimum values because minimum estimates of water depth were used. If subsidence and long-term sea-level rise were regular, this signal theoretically reflects the eustatic sea-level changes created by the orbital precession and first eccentricity cycles.

Paleogeographic Evolution

On the basis of the high-resolution correlation of the elementary sequences (Fig. 8) and the inferred high-frequency sea-level curve (Fig. 10), the paleogeographic evolution of the platform can now be reconstructed with time steps of 20 ky (Fig. 11). Although large distances separate the studied sections and the correlation of the elementary sequences is uncertain in places, the image of a stepwise transgression is evident. While the platform interior (Rusel section) is still dominated by freshwater lakes, ooid bars form at the platform edge (Salève section) and shelter lagoons from high energy (Vuache section). Washovers occasionally carry marine material into the coastal lakes at Chapeau du Gendarme.

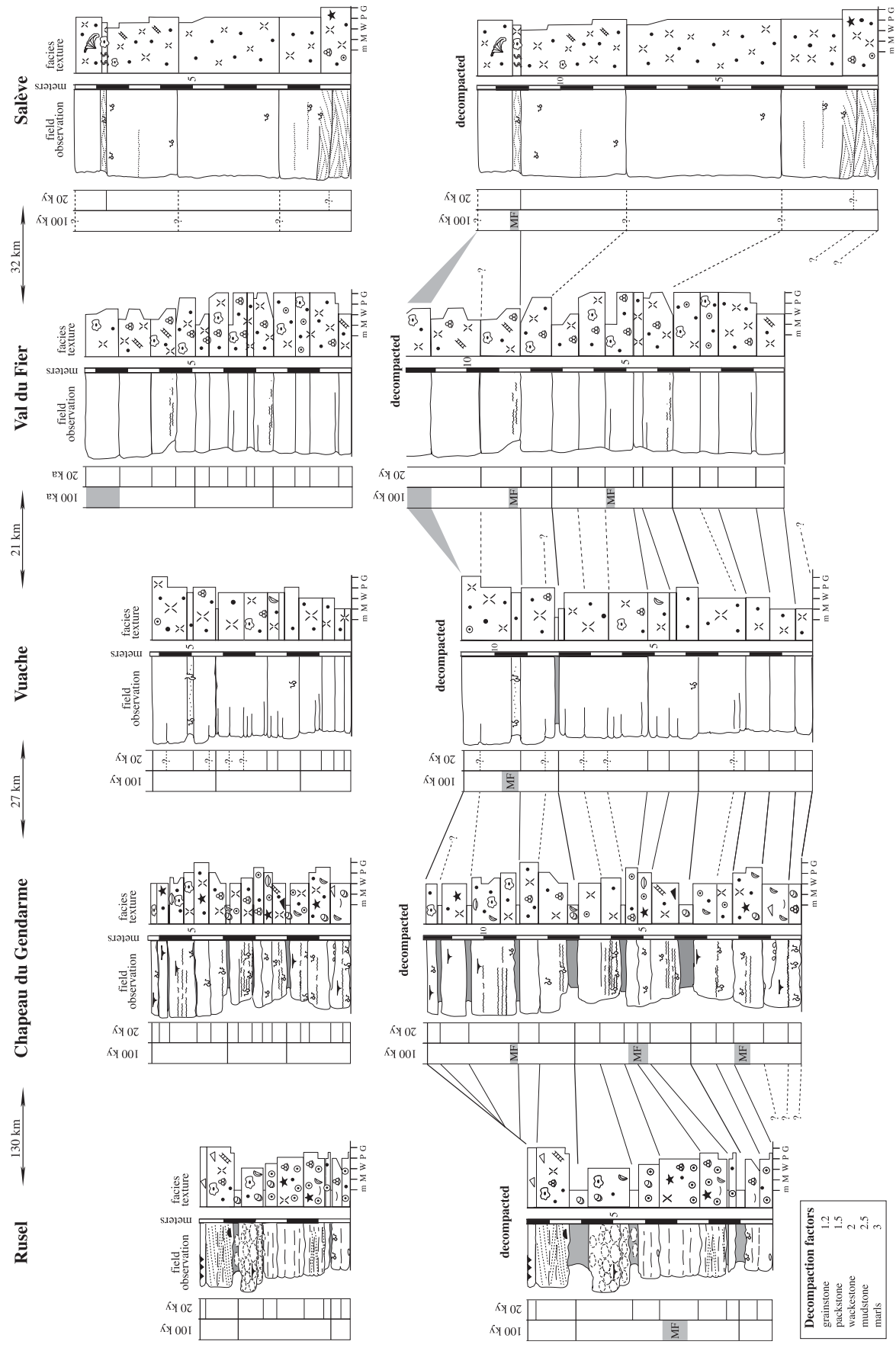

FIG. 8.—Decompaction of the lowermost three small-scale sequences of the Pierre-Châtel Formation, and best-fit correlation of the elementary sequences. The maximum-flooding interval of the third small-scale sequence is assumed to have been isochronous and is used as reference level. Symbols as in Figure 5. For discussion see text.

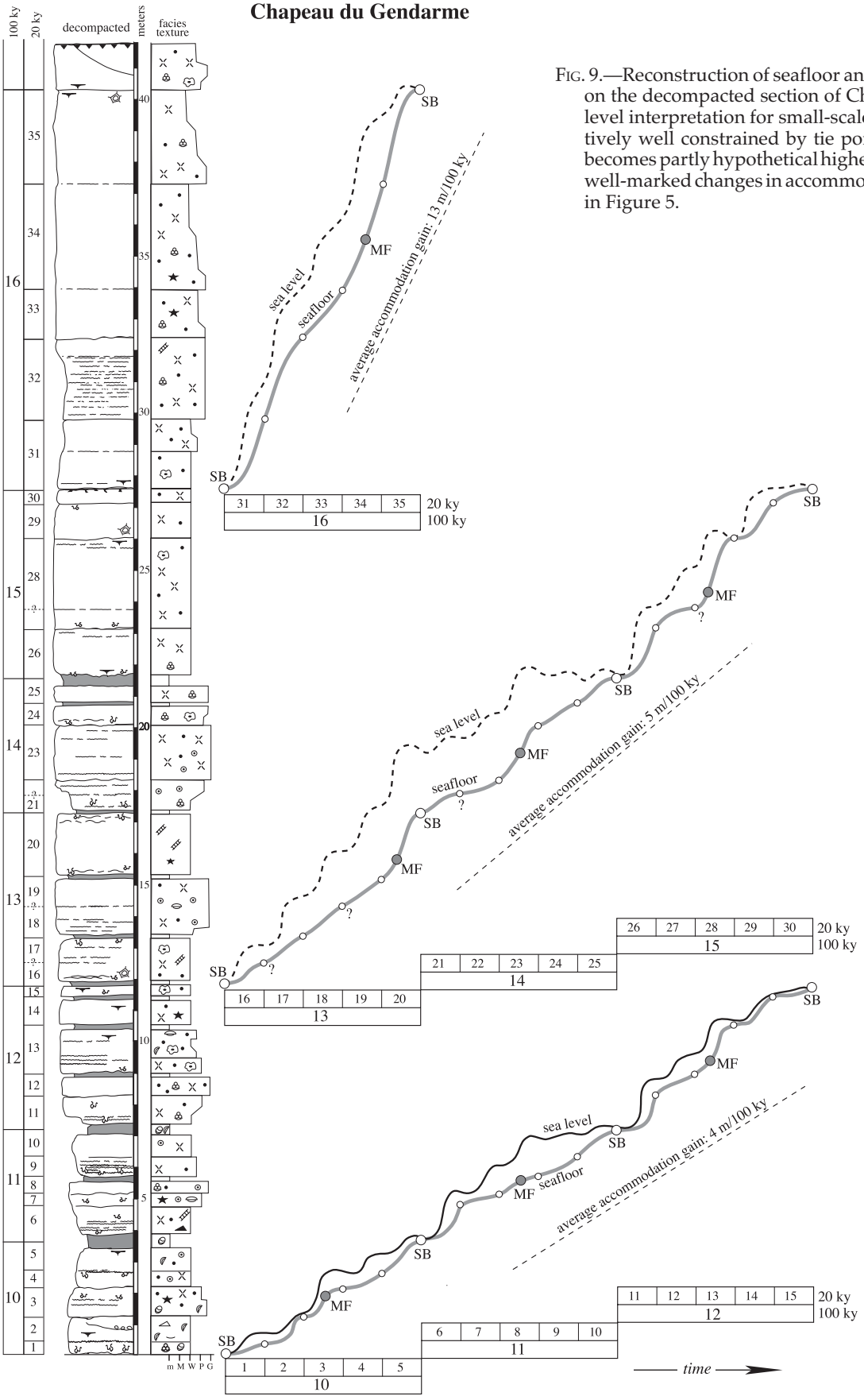

FIG. 9.—Reconstruction of seafloor and sea-level evolution based on the decompacted section of Chapeau du Gendarme. Sea-level interpretation for small-scale sequences 10 to 12 is relatively well constrained by tie points of intertidal facies but becomes partly hypothetical higher up in the section. Note the well-marked changes in accommodation gain. Symbols are as in Figure 5.

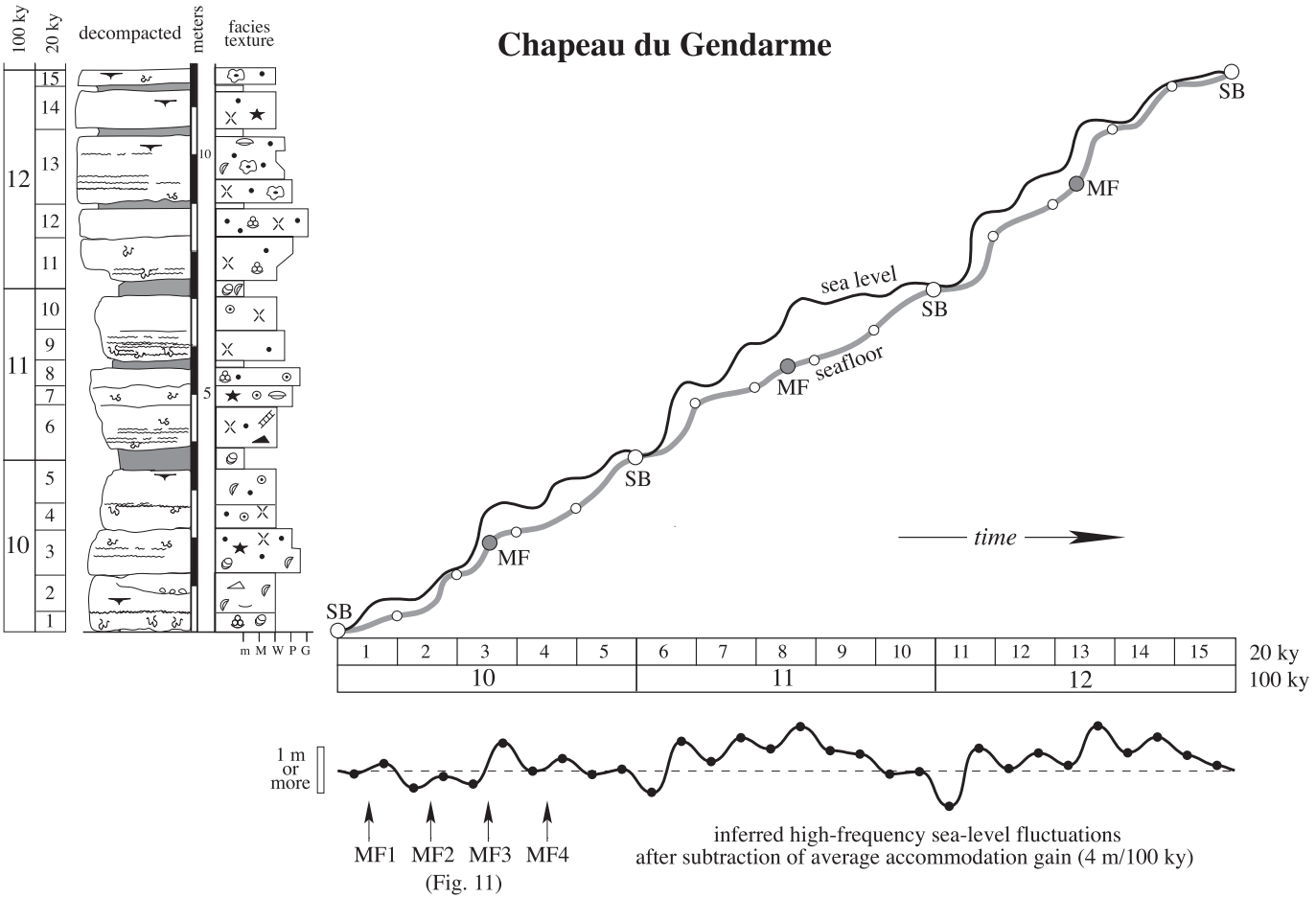

FIG. 10.—Reconstruction of a high-frequency eustatic sea-level curve from the decompacted lower part of the Chapeau-du-Gendarme section. For discussion refer to text. Symbols are as in Figure 5.

With the next transgressive pulse 20 ky later (which has a very low amplitude; Fig. 10), the situation does not change much except for a tidal flat with channels that develops at Chapeau du Gendarme. The following sea-level rise, however, is of higher amplitude and causes marine flooding of the platform as far as Chapeau du Gendarme. Rusel still keeps its lacustrine facies, and ooid shoals develop there only after the fourth transgressive pulse. Although the amplitude of this sea-level fluctuation is low, it is able to pass a threshold and establish marine conditions even in the platform interior.

DISCUSSION

Definition and Correlation of Depositional Sequences

A depositional sequence is defined by its facies evolution, which translates environmental change through time. In the studied sections, deepening–shallowing facies trends imply that accommodation changes are an important factor for sequence development. Supratidal features directly superimposed on subtidal facies cannot be produced by simple progradation of the sedimentary system and indicate that drops in relative sea level must have occurred (Hardie et al., 1986; Strasser, 1991; D'Argenio et al., 1997). The hierarchical stacking of sequences further suggests that these accommodation changes were controlled at least partly by high-frequency sea-level changes reflecting Milankovitch cyclicity.

However, if sea-level amplitudes are not high enough to induce facies changes in subtidal environments, no sequence boundaries or maximum-flooding surfaces will be recognizable. In the studied sections, beds commonly are separated by marly joints. Clays that are washed into the system during a sea-level fall may create such a marly joint and define a sequence boundary, but clays can also be mobilized through climate change, which is not necessarily in tune with sea-level change. On the other hand, clays may be concentrated because of reduced carbonate production below the photic zone or low-energy conditions below wave base. Early diagenesis commonly enhances the marl–limestone contrast through migration of carbonate from marls to limestones (Ricken and Eder, 1991). Some bedding planes created by the marls can be traced from one section to the other, others for only a few meters. Localized marl seams may reflect depressions on the seafloor where clays accumulated preferentially. The number of beds counted in a section therefore does not necessarily correspond to the number of sea-level cycles recorded.

Small-scale sequences were defined in portions of the studied sections where facies changes permit their easy identification (Fig. 4). By piecing together such portions within a rough frame given by biostratigraphy and major lithologic changes, a best-fit

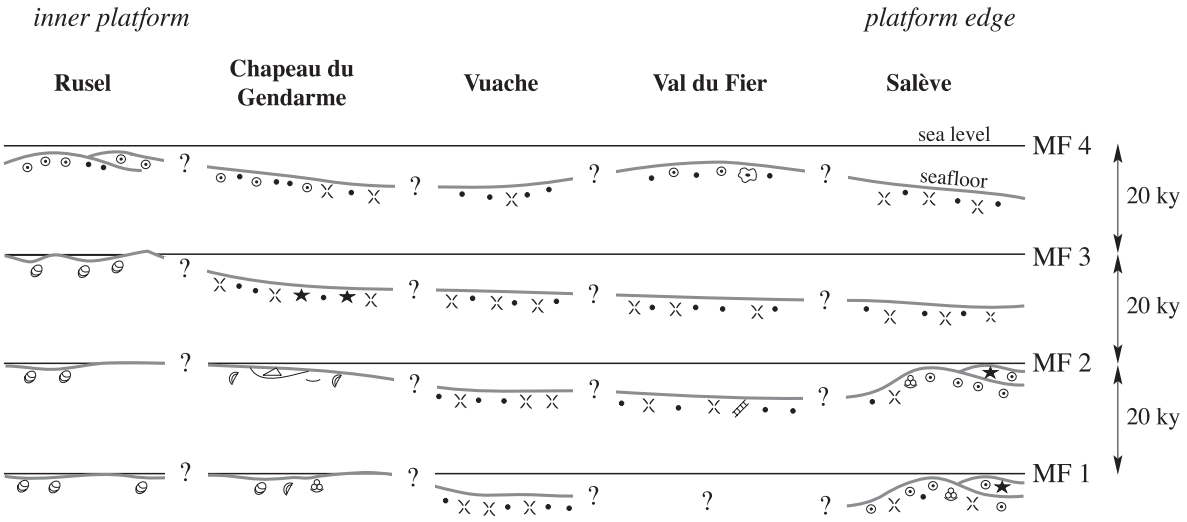

FIG. 11.—Hypothetical evolution of the Jura platform during the transgression that led to the deposition of the lower part of the Pierre-Châtel Formation. MF1 to MF4 correspond to the times of maximum flooding identified on the high-frequency sea-level curve in Figure 10. Symbols as in Figure 5. For discussion see text.

solution such as in Figure 5 can be proposed. Lateral correlation allows sequence boundaries to be inferred also in intervals where they are not clearly developed. However, especially in high-energy deposits, reactivation surfaces may simulate sequence boundaries. There, it may be easier to correlate maximum-flooding intervals (e.g., small-scale sequences 12 and 13 in the Salève section; Fig. 5).

Once the correlation is performed, and despite uncertainties in placing some small-scale sequence boundaries, it becomes clear that major lithological changes are not necessarily isochronous. For example, on the large scale (within one ammonite subzone), a major transgressive surface defines the base of the Pierre-Châtel Formation (Fig. 5). On the scale of elementary sequences, however, a stepwise flooding of the platform can be demonstrated (Figs. 8, 11).

Timing and Estimation of Sedimentation Rates

The timing of the depositional sequences defined in this study follows two lines of reasoning. First, dated ammonite zones and sequence boundaries give a rough estimate of the duration of the studied interval. Dividing this duration by the number of identified elementary and small-scale sequences places these within the Milankovitch frequency band. Second, the average of five elementary sequences building one small-scale sequence reflects the ratio between the precession cycle and the first eccentricity cycle. Medium-scale sequences, composed of four small-scale sequences and corresponding to the 400 ky eccentricity cycle, are poorly defined in the interval presented in Figure 5 but become apparent in the Upper Berriasian units (Strasser and Hillgärtner, 1998; Hillgärtner, 1999).

Uncertainties of course exist because the radiometric dating may include large error margins, and because bed thicknesses and stacking pattern do not always correspond to accommodation changes driven by sea-level fluctuations that are in tune with the Milankovitch cycles. In the platform sections, even if the sequences are differentially decompacted (e.g., Bond et al., 1993), their reconstructed thicknesses still do not reflect accommodation unless the top of the sequence shows intertidal facies. Tops of sequences may also be eroded, and erosion depth is difficult to evaluate. Estimation of water depths of subtidal facies is difficult, and error margins are large. Consequently, spectral analysis of bed thicknesses to test the Milankovitch hypothesis was not performed. In the Montclus section, slumps interrupt the limestone–marl alternations and preclude a spectral analysis based on a reasonably long time series.

It is evident from Figures 6 and 9 that the distribution of time within a sequence is not homogeneous. This is why it is difficult to estimate sedimentation rates. It is pointless to divide thickness by time because each facies may have a different production rate, because sediment may be deposited but then redistributed over the platform (e.g., Pratt and James, 1986) or exported to the basin (e.g., Schlager et al., 1994), and significant amounts of time may be spent without sediment accumulation or even with erosion, especially in the early-transgressive and late-highstand phases of a sea-level cycle (e.g., Goldhammer et al., 1990; Strasser, 1994). Consequently, one should distinguish clearly between sediment production rate, accumulation rate, and final preservation. Ancient accumulation rates are often calculated over long time intervals and indicated in meters per million years (e.g., Wilkinson et al., 1991; Bosscher and Schlager, 1993). Thus, changes in subsidence rate, hiatuses, and short-term variations in sediment production are not adequately taken into account. It is probably more realistic to estimate accumulation rates separately for each elementary or small-scale sequence.

Reconstruction of Eustatic Sea-Level Changes

On the scale of the platform studied, it can be assumed that eustatic sea-level fluctuations were synchronous. Subsidence rates, however, changed not only through time but also from one tectonic compartment to another. Assuming that the decompacted thicknesses and the correlation of the depositional sequences as presented in Figure 8 are correct, the thickness variations between Chapeau du Gendarme, Vuache, and Val du Fier appear to be minor and can be explained by changes in seafloor morphology. When the first three small-scale sequences were deposited, these sections were probably situated on the same tectonic compartment. However, the Rusel section experienced decreased subsidence or even uplift during the deposition of the

third small-scale sequence, while the Salève section expresses increased subsidence at the platform margin for the first 250 ky. The sea-level reconstruction in Figure 10 is therefore based on the Chapeau-du-Gendarme section, where the sequences are clearly marked and at least two other sections show a similar thickness evolution. Many more sections in different locations would have to be analyzed to reconstruct a sea-level curve valid for the whole platform. Unfortunately, outcrop conditions in the Swiss and French Jura are such that good sections are rare.

The only tie points for the sea-level curve ("pinning points" of Goldstein and Franseen, 1995) are intertidal or marginal-marine facies, where mean sea level is at zero. If a vadose zone is developed, sea level must have fallen at least to the base of this zone. If only subtidal facies are present at the sequence boundary, water depth at that time has to be estimated from the facies and the paleoecology of the organisms present, which generally includes wide error margins (Steinhauff and Walker, 1995). The same holds true for water depth during maximum flooding. Fischer plots have not been employed in this study because they only trace changes in sequence thickness through time (Sadler et al., 1993) and do not account for accommodation space that is not filled (Osleger, 1991; Osleger and Read, 1991).

Sea-level changes during greenhouse conditions, as in the Early Cretaceous, were of lower amplitude and probably more regular than during glaciations (e.g., Koerschner and Read, 1989). However, orbitally driven changes in insolation translate into sea-level changes through several feedback mechanisms (Gornitz et al., 1982; Schulz and Schäfer-Neth, 1998; Jacobs and Sahagian, 1993). It can be assumed that irregularities caused by complex climate–ocean coupling occurred, even if their amplitudes were certainly less than in glacioeustatically dominated times such as the Pleistocene and Holocene (e.g., Kindler and Hearty, 1996; Peltier, 1988). Such irregularities could have led to facies changes that may simulate a Milankovitch cycle.

Potential of the Cyclostratigrapical Approach

Despite the uncertainties mentioned above, cyclostratigraphic analysis of carbonate platforms can greatly improve the understanding of their functioning. It is seen that the general trends of long-term (million-year scale) tectonic, climatic, and eustatic sea-level changes do not directly control the sedimentation but rather give the baseline for high-frequency environmental changes which are, directly or indirectly, linked to the orbital insolation changes. If Milankovitch cyclicity can be demonstrated, the duration of the observed depositional sequences is known. On the basis of detailed facies analysis, the rates of sedimentary, ecological, and diagenetic processes can then be estimated. Because the time intervals within which these processes are studied are relatively short (20 to 100 ky), a comparison with Pleistocene and Holocene rates can be made, where relevant data are much more abundant (e.g., Enos, 1991). Of course, it has to be considered that amplitudes of climate change and sea-level change differed greatly between greenhouse and icehouse worlds.

For example, during the first 300 ky of the transgression studied on the Jura platform, less than 2 m of sediment were preserved per 20 ky. In contrast, Holocene production rates of comparable lagoonal–peritidal facies are considerably higher (potentially 4 to 20 m in 20 ky; Enos, 1991). It is therefore suggested that sediment production is active during only part of a 20 ky cycle. A sea-level drop may cause erosion and subaerial exposure, and sediment production may need some time to start up when sea level rises again. Changes in climate periodically increase runoff of clays and nutrients from the hinterland, which hampers carbonate production (Hallock and Schlager, 1986). Also, part of the produced sediment is redistributed on the platform by currents and storms and exported towards the basin (e.g., Milliman et al., 1993).

The cyclostratigraphic approach further allows estimation of the time represented in stratigraphic gaps. In the Salève section, the 50 cm interval between sequence boundary Be4 and the transgressive surface at the base of the Pierre-Châtel Formation probably represents about 900 ky (Fig. 5). The karst surface underlining SB Be5 represents at least 300 ky in the section of Rusel, and at least 150 ky at Chapeau du Gendarme (Fig. 5).

The cyclostratigraphic analysis thus refines sequence-stratigraphic correlations. This has been demonstrated for sections on the platform (e.g., Goldhammer et al., 1994; D'Argenio et al., 1997; D'Argenio et al., 1999; Chen et al., 2001; Raspini, 2001) and for correlations from platform to ramp and basin (e.g., Elrick and Read, 1991; Pasquier and Strasser, 1997; Osleger, 1998; Pittet and Strasser, 1998; Betzler et al., 1999). The evolution of the sedimentary systems can be monitored in time steps of 20 or 100 ky, and this independently of the error margins of absolute dating.

CONCLUSIONS

Analysis of facies evolution and stacking pattern of depositional sequences in the Berriasian of the Swiss and French Jura Mountains suggests that high-frequency eustatic sea-level changes were an important factor controlling sedimentation on the shallow carbonate platform. Elementary and small-scale sequences are recognized. The biostratigraphic, sequence-stratigraphic, and cyclostratigraphic correlation with a well-dated deeper-water section implies that these sequences formed in tune with the 20 ky and 100 ky orbital cycles.

Three small-scale sequences constituting the early transgressive interval of the Pierre-Châtel Formation were analyzed in detail. Facies-dependent decompaction and correlation of the elementary sequences indicates that differential subsidence led to episodic accommodation changes. It also shows that the transgression flooded the platform in pulses: every 20 ky, marine conditions reached farther into the platform interior.

The reconstruction of a high-frequency sea-level curve cannot be more than a rough approximation but nevertheless opens the way to discuss rates of sediment production and accumulation on a scale that is comparable to that of the Pleistocene and the Holocene. This high time resolution also offers a potential to estimate rates of paleoecological and diagenetic processes.

However, considering the complexity of any sedimentary system, considering the multiple mechanisms that translate orbitally controlled insolation changes into sea-level fluctuations as well as into climatic and ecological changes at a given paleogeographical position, and considering the incompleteness of the sedimentary record, great care has to be taken in the interpretations. It is impossible to generalize from one study in one time interval and one paleogeographical and geodynamic setting. Cyclostratigraphy is a valuable tool that helps to establish a narrow time frame, but estimation of time involved in sedimentary processes also calls for detailed bed-by-bed analyses in order to understand the functioning of the corresponding depositional environments.

ACKNOWLEDGMENTS

Many of the ideas presented here have been elaborated together with Bernard Pittet, Christophe Dupraz, Wolfgang Hug, and Alex Waehry. We thank them for the animated discussions. We also thank Élias Samankassou for critically reading a first version of the manuscript. The constructive remarks of Hanspeter

Funk and an anonymous reviewer were greatly appreciated. The financial support of this research by the Swiss National Science Foundation (project No. 20-56491.99) is gratefully acknowledged.

REFERENCES

Bathurst, R.G.C., 1987, Diagenetically enhanced bedding in argillaceous platform limestones: stratified cementation and selective compaction: Sedimentology, v. 34, p. 749–778.

Berger, A., Loutre, M.F., and Dehant, V., 1989, Astronomical frequencies for pre-Quaternary palaeoclimate studies: Terra Nova, v. 1, p. 474–479.

Berggren, W.A., Kent, D.V., Aubry, M.P., and Hardenbol, J., eds., 1995, Geochronology, Time Scales and Global Stratigraphic Correlation: SEPM, Special Publication 54, 386 p.

Betzler, C., Reijmer, J.J.G., Bernet, K., Eberli, G.P., and Anselmetti, F.S., 1999, Sedimentary patterns and geometries of the Bahamian outer carbonate ramp (Miocene–Lower Pliocene, Great Bahama Bank): Sedimentology, v. 46, p. 1127–1143.

Blondel, T., 1984, Etude géologique de la partie septentrionale de la Montagne du Vuache (Haute Savoie—France): Unpublished Diploma Thesis, University of Geneva, 310 p.

Bond, G.C., Devlin, W.J., Kominz, M.A., Beavan, J., and McManus, J., 1993, Evidence of astronomical forcing of the Earth's climate in Cretaceous and Cambrian times: Tectonophysics, v. 222, p. 295–315.

Bosscher, H., and Schlager, W., 1993, Accumulation rates of carbonate platforms: Journal of Geology, v. 101, p. 345–355.

Chen, D., Tucker, M.E, Jiang, M., and Zhu, J., 2001, Long-distance correlation between tectonic-controlled, isolated carbonate platforms by cyclostratigraphy and sequence stratigraphy in the Devonian of South China: Sedimentology, v. 48, p. 57–78.

Clavel, B., Charollais, J., Busnardo, R., and Le Hegarat, G., 1986, Précisions stratigraphiques sur le Crétacé inférieur basal du Jura méridional: Eclogae Geologicae Helvetiae, v. 79, p. 319–341.

Cotillon, P., Ferry, S., Gaillard, C., Jautée, E., Latreille, G., and Rio, M., 1980, Fluctuation des paramètres du milieu marin dans le domaine vocontien (France Sud-Est) au Crétacé inférieur: mise en évidence par l'étude des formations marno-calcaires alternantes: Société Géologique de France, Bulletin, v. 7/22, p. 735–744.

Darsac, C., 1983, La plate-forme berriaso-valanginienne du Jura méridional aux massifs subalpins (Ain, Savoie): Ph.D. Dissertation, University of Grenoble, 319 p.

D'Argenio, B., Ferreri, V., Amodio, S., and Pelosi, N., 1997, Hierarchy of high-frequency orbital cycles in Cretaceous carbonate platform strata: Sedimentary Geology, v. 113, p. 169–193.

D'Argenio, B., Ferreri, V., Raspini, A., Amodio, S., and Buonocunto, F.P., 1999, Cyclostratigraphy of a carbonate platform as a tool for high-precision correlation: Tectonophysics, v. 315, p. 357–385.

De Graciansky, P.-C., and Lemoine, M., 1988, Early Cretaceous extensional tectonics in the southwestern French Alps: a consequence of North-Atlantic rifting during Tethyan spreading: Société Géologique de France, Bulletin, v. 8/4, p. 733–737.

Dercourt, J., Gaetani, M., Vrielynck, B., Barrier, E., Biju-Duval, B., Brunet, M.F., Cadet, J.P., Crasquin, S., and Sandulescu, M., eds., 2000, Atlas Peri-Tethys—Palaeogeographical Maps: Paris.

Détraz, H., and Mojon, P.-O., 1989, Evolution paléogéographique de la marge jurassienne de la Téthys du Tithonique–Portlandien au Valanginien: corrélations biostratigraphique et séquentielle des faciès marins à continentaux: Eclogae Geologicae Helvetiae, v. 82, p. 37–112.

Einsele, G., and Ricken, W., 1991, Limestone–marl alternation—an overview, *in* Einsele, G., Ricken, W., and Seilacher, A., eds., Cycles and Events in Stratigraphy: Berlin, Springer-Verlag, p. 23–47.

Elrick, M., and Read, J.F., 1991, Cyclic ramp-to-basin carbonate deposits, Lower Mississippian, Wyoming and Montana: a combined field and computer study: Journal of Sedimentary Petrology, v. 61, p. 1194–1224.

Enos, Paul, 1991, Sedimentary parameters for computer modeling, *in* Franseen, E.K., Watney, W.L., Kendall, C.G.St.C., and Ross, W., eds., Sedimentary Modeling: Computer Simulations and Methods for Improved Parameter Definition: Kansas Geological Survey, Memoir 233, p. 63–99.

Eyles, N., 1993, Earth's glacial record and its tectonic setting: Earth-Science Reviews, v. 35, p. 1–248.

Fairbridge, R.W., 1976, Convergence of evidence on climatic change and ice ages: New York Academy of Science, Annals, v. 91, p. 542–579.

Frakes, L.A., Francis, J.E., and Syktus, J.I., 1992, Climate Modes of the Phanerozoic: Cambridge, U.K., Cambridge University Press, 274 p.

Goldhammer, R.K., 1997, Compaction and decompaction algorithms for sedimentary carbonates: Journal of Sedimentary Research, v. 67, p. 26–35.

Goldhammer, R.K., Dunn, P.A., and Hardie, L.A., 1990, Depositional cycles, composite sea-level changes, cycle stacking patterns, and the hierarchy of stratigraphic forcing: Examples from Alpine Triassic platform carbonates: Geological Society of America, Bulletin, v. 102, p. 535–562.

Goldhammer, R.K., Oswald, E.J., and Dunn, P.A., 1994, High-frequency, glacio-eustatic cyclicity in the Middle Pennsylvanian of the Paradox Basin: an evaluation of Milankovitch forcing, *in* de Boer, P.L., and Smith, D.G., eds., Orbital Forcing and Cyclic Sequences: International Association of Sedimentologists, Special Publication 19, p. 243–283.

Goldstein, R.H., and Franseen, E.K., 1995, Pinning points: a method providing quantitative constraints on relative sea-level history: Sedimentary Geology, v. 95, p. 1–10.

Gornitz, V., Lebedeff, S., and Hansen, J., 1982, Global sea-level trend in the past century: Science, v. 215, p. 1611–1614.

Gradstein, F.M., Agterberg, F.P., Ogg, J.G., Hardenbol, J., van Veen, P., Thierry, J., and Huang, Z., 1995, A Triassic, Jurassic and Cretaceous time scale, *in* Berggren, W.A., Kent, D.V., Aubry, M.P., and Hardenbol, J., eds., Geochronology, Time Scales and Global Stratigraphic Correlation: SEPM, Special Publication 54, p. 95–126.

Häfeli, C., 1966, Die Jura/Kreide-Grenzschichten im Bielerseegebiet (Kt. Bern): Eclogae Geologicae Helvetiae, v. 59, p. 565–696.

Halley, R.B., and Harris, P.M., 1979, Fresh-water cementation of a 1,000-year-old oolite: Journal of Sedimentary Petrology, v. 49, p. 969–988.

Hallock, P., and Schlager, W., 1986, Nutrient excess and the demise of coral reefs and carbonate platforms: Palaios, v. 1, p. 389–398.

Hardenbol, J., Thierry, J., Farley, M.B., Jacquin, T., de Graciansky, P.-C., and Vail, P.R., 1998, Charts, *in* de Graciansky, P.-C., Hardenbol, J., Jacquin, T., and Vail, P.R., eds., Mesozoic and Cenozoic Sequence Stratigraphy of European Basins: SEPM, Special Publication 60.

Hardie, L.A., Bosellini, A., and Goldhammer, R.K., 1986, Repeated subaerial exposure of subtidal carbonate platforms, Triassic, Northern Italy: evidence for high frequency sea level oscillations on a 10^4 year scale: Paleoceanography, v. 1, p. 447–457.

Hillgärtner, H., 1999, The evolution of the French Jura platform during the Late Berriasian to Early Valanginian: controlling factors and timing: GeoFocus, v. 1, 203 p.

Jacobs, D.K., and Sahagian, D.L., 1993, Climate-induced fluctuations in sea level during non-glacial times: Nature, v. 361, p. 710–712.

Jacquin, T., and de Graciansky, P.-C., 1998, Transgressive/regressive (second order) facies cycles: the effects of tectono-eustasy, *in* de Graciansky, P.-C., Hardenbol, J., Jacquin, T., and Vail, P.R., eds., Mesozoic and Cenozoic Sequence Stratigraphy of European Basins: SEPM, Special Publication 60, p. 31–42.

Kindler, P., and Hearty, P.J., 1996, Carbonate petrography as an indicator of climate and sea-level changes: new data from Bahamian Quaternary units: Sedimentology, v. 43, p. 381–399.

Koerschner, W.F., III, and Read, J.F., 1989, Field and modelling studies of Cambrian carbonate cycles, Virginia Appalachians: Journal of Sedimentary Petrology, v. 59, p. 654–687.

LE HEGARAT, G., 1971, Le Berriasien du Sud-Est de la France: Université de Lyon, Faculté des Sciences, Laboratoire Géologique, Documents, v. 43, 576 p.

LOURENS, L.J., ANTONARAKOU, A., HILGEN, F.J., VAN HOOF, A.A.M., VERGNAUD-GRAZZINI, C., AND ZACHARIASSE, W.J., 1996, Evaluation of the Plio-Pleistocene astronomical timescale: Paleoceanography, v. 11, p. 391–413.

MEYER, M., 2000, Le complexe récifal kimméridgien–tithonien du Jura méridional interne (France), évolution multifactorielle, stratigraphie et tectonique: Terre & Environnement, v. 24, 179 p.

MILLIMAN, J.D., FREILE, D., STEINEN, R.P., AND WILBER, R.J., 1993, Great Bahama Bank aragonite muds: mostly inorganically precipitated, mostly exported: Journal of Sedimentary Petrology, v. 63, p. 589–595.

MONTAÑEZ, I.P., AND OSLEGER, D.A., 1993, Parasequence stacking patterns, third-order accommodation events, and sequence stratigraphy of Middle to Upper Cambrian platform carbonates, Bonanza King Formation, southern Great Basin, *in* Loucks R.G., and Sarg, J.F., eds., Carbonate Sequence Stratigraphy: American Association of Petroleum Geologists, Memoir 57, p. 305–326.

MOORE, C.H., 1989, Carbonate Diagenesis and Porosity: Amsterdam, Elsevier, Developments in Sedimentology, v. 46, 338 p.

OSLEGER, D.A., 1991, Subtidal carbonate cycles: Implications for allocyclic vs. autocyclic controls: Geology, v. 19, p. 917–920.

OSLEGER, D.A., 1998, Sequence architecture and sea-level dynamics of Upper Permian shelfal facies, Guadalupe Mountains, southern New Mexico: Journal of Sedimentary Research, v. 68, p. 327–346.

OSLEGER, D., AND READ, J.F., 1991, Relation of eustasy to stacking pattern of meter-scale carbonate cycles, Late Cambrian, U.S.A.; Journal of Sedimentary Petrology, v. 61, p. 1225–1252.

PASQUIER, J.-B., 1995, Sédimentologie, stratigraphie séquentielle et cyclostratigraphie de la marge nord-thétysienne au Berriasien en Suisse occidentale (Jura, Helvétique et Ultrahelvétique; comparaison avec les séries de bassin des domaines vocontien et subbriançonnais): Ph.D. Dissertation, University of Fribourg, 274 p.

PASQUIER, J.-B., AND STRASSER, A., 1997, Platform-to-basin correlation by high-resolution sequence stratigraphy and cyclostratigraphy (Berriasian, Switzerland and France): Sedimentology, v. 44, p. 1071–1092.

PELTIER, W.R., 1988, Lithospheric thickness, Antarctic deglaciation history, and ocean basin discretization effects in a global model of postglacial sea-level change: a summary of some sources of nonuniqueness: Quaternary Research, v. 29, p. 93–112.

PITTET, B., AND STRASSER, A., 1998, Long-distance correlations by sequence stratigraphy and cyclostratigraphy: examples and implications (Oxfordian from the Swiss Jura, Spain, and Normandy): Geologische Rundschau, v. 86, p. 852–874.

PITTET, B., STRASSER, A., AND MATTIOLI, E., 2000, Depositional sequences in deep-shelf environments: a response to sea-level changes and shallow-platform carbonate productivity (Oxfordian, Germany and Spain): Journal of Sedimentary Research, v. 70, p. 392–407.

PRATT, B.R., AND JAMES, N.P., 1986, The St George Group (Lower Ordovician) of western Newfoundland: tidal flat island model for carbonate sedimentation in shallow epeiric seas: Sedimentology, v. 33, p. 313–343.

PRICE, G.D., 1999, The evidence and implications of polar ice during the Mesozoic: Earth-Science Reviews, v. 48, p. 183–210.

RASPINI, A., 2001, Stacking pattern of cyclic carbonate platform strata: Lower Cretaceous of southern Apennines, Italy: Geological Society of London, Journal, v. 158, p. 353–366.

RICKEN, W., AND EDER, W., 1991, Diagenetic modification of calcareous beds—an overview, *in* Einsele, G., Ricken, W., and Seilacher, A., eds., Cycles and Events in Stratigraphy: Berlin, Springer-Verlag, p. 430–449.

SADLER, P.M., OSLEGER, D.A., AND MONTAÑEZ, I.P., 1993, On the labeling, length, and objective basis of Fischer plots: Journal of Sedimentary Petrology, v. 63, p. 360–368.

SCHLAGER, W., REIJMER, J.J.G., AND DROXLER, A., 1994, Highstand shedding of carbonate platforms: Journal of Sedimentary Research, v. B64, p. 270–281.

SCHULZ, M., AND SCHÄFER-NETH, C., 1998, Translating Milankovitch climate forcing into eustatic fluctuations via thermal deep water expansion: a conceptual link: Terra Nova, v. 9, p. 228–231.

SCHWARZACHER, W., 1993, Cyclostratigraphy and the Milankovitch Theory: Amsterdam, Elsevier, Developments in Sedimentology, v. 52, 225 p.

SHINN, E.A., AND ROBBIN, D.M., 1983, Mechanical and chemical compaction in fine-grained shallow-water limestones: Journal of Sedimentary Petrology, v. 53, p. 595–618.

SINCLAIR, I.K., SHANNON, P.M., WILLIAMS, B.P.J., HARKER, S.D., AND MOORE, J.G., 1994, Tectonic control on sedimentary evolution of three North Atlantic borderland Mesozoic basins: Basin Research, v. 6, p. 193–217.

STEINHAUFF, D.M., AND WALKER, K.R., 1995, Recognizing exposure, drowning, and "missed beats": platform-interior to platform-margin sequence stratigraphy of Middle Ordovician limestones, east Tennessee: Journal of Sedimentary Research, v. B65, p. 183–207.

STEINHAUSER, N., AND LOMBARD, A., 1969, Définition de nouvelles unités lithostratigraphiques dans le Crétacé inférieur du Jura méridional (France): Société Physique et Histoire Naturelle, Genève, Comptes Rendus, v. 4, p. 100–113.

STRASSER, A., 1988, Shallowing-upward sequences in Purbeckian peritidal carbonates (lowermost Cretaceous, Swiss and French Jura Mountains): Sedimentology, v. 35, p. 369–383.

STRASSER, A., 1991, Lagoonal–peritidal sequences in carbonate environments: autocyclic and allocyclic processes, *in* Einsele, G., Ricken W., and Seilacher, A., eds., Cycles and Events in Stratigraphy: Berlin, Springer-Verlag, p. 709–721.

STRASSER, A., 1994, Milankovitch cyclicity and high-resolution sequence stratigraphy in lagoonal–peritidal carbonates (Upper Tithonian–Lower Berriasian, French Jura Mountains), *in* de Boer, P.L., and Smith, D.G., eds., Orbital Forcing and Cyclic Sequences: International Association of Sedimentologists, Special Publication 19, p. 285–301.

STRASSER, A., AND DAVAUD, E., 1983, Black pebbles of the Purbeckian (Swiss and French Jura): lithology, geochemistry and origin: Eclogae Geologicae Helvetiae, v. 76, p. 551–580.

STRASSER, A., AND HILLGÄRTNER, H., 1998, High-frequency sea-level fluctuations recorded on a shallow carbonate platform (Berriasian and Lower Valanginian of Mount Salève, French Jura): Eclogae Geologicae Helvetiae, v. 91, p. 375–390.

STRASSER, A., PITTET, B., HILLGÄRTNER, H., AND PASQUIER, J.-B., 1999, Depositional sequences in shallow carbonate-dominated sedimentary systems: concepts for a high-resolution analysis: Sedimentary Geology, v. 128, p. 201–221.

STRASSER, A., HILLGÄRTNER, H., HUG, W., AND PITTET, B., 2000, Third-order depositional sequences reflecting Milankovitch cyclicity: Terra Nova, v. 12, p. 303–311.

STROHMENGER, C., AND STRASSER, A., 1993, Eustatic controls on the depositional evolution of Upper Tithonian and Berriasian deep-water carbonates (Vocontian Trough, SE France): Centres Recherche Exploration-Production Elf Aquitaine, Bulletin, v. 17, p. 183–203.

TRÜMPY, R., 1980, Geology of Switzerland, a Guide-Book. Part A: An Outline of the Geology of Switzerland: Basel, Wepf & Co. Publishers, 104 p.

VAIL, P.R., AUDEMARD, F., BOWMAN, S.A., EISNER, P.N., AND PEREZ-CRUZ, C., 1991, The stratigraphic signatures of tectonics, eustasy and sedimentology—an overview, *in* Einsele, G., Ricken W., and Seilacher, A., eds., Cycles and Events in Stratigraphy: Berlin, Springer-Verlag, p. 617–659.

WAEHRY, A., 1989, Faciès et séquences de dépôt dans la Formation de Pierre-Châtel (Berriasien moyen, Jura méridional / France): Unpublished Diploma Thesis, University of Geneva, 83 p.

WILDI, W., FUNK, H., LOUP, B., AMATO, E., AND HUGGENBERGER, P., 1989, Mesozoic subsidence history of the European marginal shelves of the Alpine Tethys (Helvetic realm, Swiss Plateau and Jura): Eclogae Geologicae Helvetiae, v. 82, p. 817–840.

WILKINSON, B.H., OPDYKE, B.N., AND ALGEO, T.J., 1991, Time partitioning in cratonic carbonate rocks: Geology, v. 19, p. 1093–1096.
ZIEGLER, P.A., 1988, Evolution of the Arctic–North Atlantic and the Western Tethys: American Association of Petroleum Geologists, Memoir 43, 198 p.

Society for Sedimentary Geology

Membership Application

546

Personal Information:

Last Name, First (Given) Middle Initial Date of Birth

Preferred Mailing Address

City State/Province Postal Code

Country Phone Number

Fax Number Citizenship E-mail Address

Academic Record:

From	To	Institution	Major	Degree/Date

Professional Record:

From	To	Employer	Address	Nature of Work

Affiliations:

☐ AAPG ☐ AGU
☐ PS ☐ GSA
☐ IAS ☐ Other: _____

References:

① _____
Name

_____
Address

② _____
Name

_____
Address

membership type:

☐ Sustaining Member $300
Financial support may be dedicated to a specific program.

☐ Voting Member ..... see Journal Choice
Requires 3 years professional experience past bachelors degree.

☐ Associate Member ..... see Journal Choice
Waives professional experience. May not vote or hold office.

☐ Spouse Member $25
Membership at same address without additional journal.

Journal Choice:

☐ Journal of Sedimentary Research
☐ Print: $75 ☐ Online: $70 ☐ Both: $85

☐ PALAIOS
☐ Print: $75 ☐ Online: $70 ☐ Both: $85

☐ Both Journals
☐ Print: $120 ☐ Online: $110 ☐ Both: $130

☐ Add $10 surcharge to defray mailing outside the USA

Payment Information:

☐ check/money order enclosed Total Amount: _____

☐ bill my credit card

☐ Visa ☐ American Express ☐ MasterCard

Account Number: _____

Expiration Date: _____

Printed Name: _____

Signature: _____

Fax this form with credit card information to:
918.621.1685

or mail with payment to:
SEPM Membership
6128 E. 38th Street, #308
Tulsa, OK 74135, USA